Available online at www.sciencedirect.com
ScienceDirect
Surface Science 600 (2006) 3266–3273
SURFACE SCIENCE
www.elsevier.com/locate/susc

Growth and surface alloying of Fe on Pt(997)

Tae-Yon Lee, Samuel Sarbach, Klaus Kuhnke *, Klaus Kern

Max-Planck-Institut für Festkörperforschung, Heisenbergstrasse 1, D-70569 Stuttgart, Germany

Received 22 September 2005; accepted for publication 13 June 2006
Available online 30 June 2006

Abstract

The growth of ultra-thin layers of Fe on the vicinal Pt(997) surface is studied by thermal energy He atom scattering (TEAS) and Auger Electron Spectroscopy (AES) in the temperature range between 175 K and 800 K. We find three distinct regimes of qualitatively different growth type. Below 450 K the formation of a smooth first monolayer, at and above 600 K the onset of bulk alloy formation, and at intermediate temperature 500–550 K the formation of a surface alloy. Monatomic Fe rows are observed to decorate the substrate steps between 175 K and 500 K. The importance of the high step density is discussed with respect to the promotion of smooth layer growth and with respect to the alloying process and its kinetics.

Keywords: Growth; Surface diffusion; Platinum; Vicinal single crystal surfaces; Iron; Alloys; Atom–solid scattering and diffraction–elastic

1. Introduction

The preparation of FePt alloy films is of substantial interest for the study of magnetic materials, both from the fundamental and applied point of view. The magnetic properties of thin FePt alloy films, such as a high coercivity, high saturation magnetization, and a large perpendicular anisotropy, are favorable with respect to further storage device miniaturization. Alloys with alternatingly stacked Pt and Fe monolayers (based on a $L1_0$ ordering with a fcc (100) surface orientation or $L1_1$ ordering with a fcc (111) surface) are the subject of intense research with the focus on their preparation and their morphological [1] and magnetic [2] properties. Numerous studies on such systems with comparatively large thickness as well as studies of iron oxides [3,4] on Pt(111) have been published. There are, however, only few studies which address separately the Fe ultrathin film growth on Pt(111) surfaces [5], the growth on surfaces vicinal to Pt(111) [6] or the conditions for surface alloy formation [7,8]. The growth of ultrathin layers on a vicinal surface exhibits several advantages compared to low index surfaces with respect to morphology and alloying. First, true one and two-dimensional structures can be formed by step-edge decoration, suppressed island nucleation on terraces and forced layer-by-layer growth. Second, alloying can be promoted due to a facilitated intermixing near step-edges.

Another aspect makes the system important. It forms a basis for future studies of a bulk-ferromagnetic material on a template surface to create nanometer sized patterns. Such structures have attracted much attention with respect to fundamental questions of magnetism at low dimensions [9,10]. They are a means to study the origin and size dependence of magnetic properties at the nanometer limit, coupling to the substrate and magnetic anisotropy in reduced dimensions. It can be expected that a wealth of structures which can be obtained for FePt alloys allows to learn more on fundamental magnetic properties.

In this paper we study the growth of Fe on Pt(997) in the range of 0–2 ML in situ (i.e. during deposition) by thermal energy He scattering. The vicinal Pt(997) surface is employed as a template for Fe deposition. The investigation covers a wide temperature range from 200 K to 800 K. Within this range the transition from Fe epitaxial growth to surface alloying and further to bulk alloying

* Corresponding author. Tel.: +49 711 689 1454; fax: +49 711 689 1079.
E-mail address: K.Kuhnke@fkf.mpg.de (K. Kuhnke).

0039-6028/$ - see front matter © 2006 Elsevier B.V. All rights reserved.
doi:10.1016/j.susc.2006.06.014

can be observed. We describe the properties of these phases and the temperature ranges in which they can be obtained.

The paper is organized as follows: The experimental aspects of the study are presented in Section 2. The measurements by thermal energy He atom scattering (TEAS) and Auger electron spectroscopy (AES) are presented in Section 3. The subsections deal with the low temperature growth (Section 3.1) and the medium and high temperature growth (Section 3.2) separately as the latter involves different aspects of Pt–Fe alloying. Kinetic aspects of alloying are discussed in Section 3.3. The paper is summarized in Section 4.

2. Experimental

The TEAS experiments are carried out in ultra-high vacuum at a base pressure below 2×10^{-10} mbar. The set-up allows to select a wide range of scattering geometries so that He diffraction can be studied both at grazing scattering geometry which is sensitive to the step region of the surface and at non-grazing geometry which provides information on processes on the terraces [11]. Fig. 1 presents a schematic drawing of the He beam and defines the angles as they are used to describe the scattering geometry with respect to the surface orientation. The He nozzle source is cooled by a cold finger. The wavelength of the He supersonic beam is stabilized at $\lambda = 0.101$ nm for all measurements shown in this paper. The scattering chamber contains in addition an electron beam bombardment evaporator for Fe evaporation in the He scattering position and a cylindrical mirror Auger spectrometer (Omicron CMA 100) which is employed after rotating the sample and shifting it from the evaporation position. In addition, low energy electron diffraction (LEED) is available as an analytical tool.

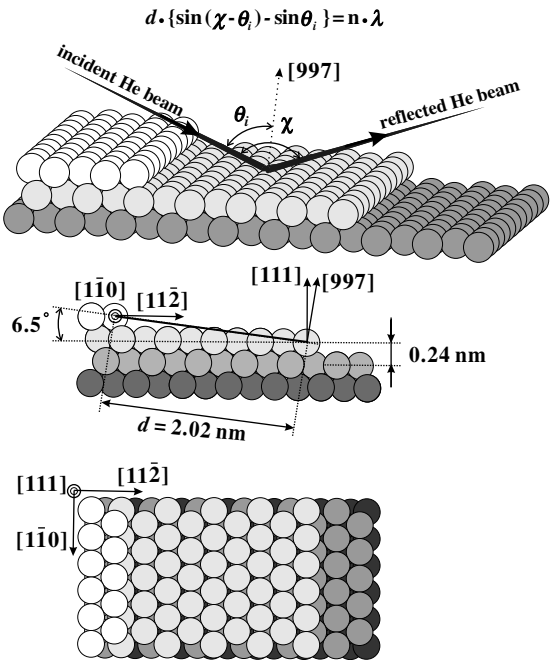

Fig. 1. Sketch of the atomic arrangement of atoms on Pt(997) in side view (center) and top view (bottom). Definition of incident angle θ_i and total scattering angle χ in He atom scattering with respect to the macroscopic surface plane (top). The Bragg formula describes the position of diffraction peaks of order n for a given He wavelength λ and surface periodicity d.

The clean Pt(997) surface is prepared by repeated cycles of 1 keV Ar^+ sputtering at 750 K surface temperature and annealing at 850 K. A low cooling rate (<40 K/min) is used after annealing so that defects (kinks) thermally created at high temperature do not freeze in. The cleanliness of the surface is checked by AES. The successful preparation of the clean substrate with high order and low defect concentration is verified by the reproducibility of absolute peak intensities and widths in the He diffraction scans. Fe is evaporated from an electron bombardment evaporator (Omicron single EFM evaporator) loaded with a 99.99% purity Fe-rod. No measures are taken to remove fast ions from the evaporation beam. Small changes of the monitored flux during evaporation are compensated by adjustment of heating power. The evaporation rate is daily calibrated by the first helium reflectivity maximum at 200 K surface temperature. This maximum is assigned to the unit 1 monolayer (ML) attributable to a full coverage of the terraces by a monatomic Fe layer (see Section 3). The employed deposition rates are typically 0.1 ML/min at a background pressure of 3×10^{-10} mbar.

Fig. 1 shows a sketch of the ideal surface geometry. Closed-packed terraces (2.02 nm wide) are separated by steps with a (1 1 1) microfacet of one monolayer height, also called B-type steps. A well-prepared surface exhibits a distribution of step–step distances with a maximum near 8 close-packed atomic rows and a standard deviation of 1 row. The properties of the Pt(997) vicinal surface and the resulting He diffraction pattern have been described in detail elsewhere [12].

3. Results and discussion

3.1. Epitaxial Fe growth on Pt(997)

Fig. 2 shows the reflected He diffraction intensity in grazing scattering geometry measured in situ during Fe deposition in the substrate temperature range $175\ \mathrm{K} \leqslant T \leqslant 800\ \mathrm{K}$. Scattering in grazing incidence geometry is extremely sensitive to the defect (kink) density at step-edges. For pseudomorphic growth the average terrace on the Pt(997) surface provides space for 8 close-packed adsorbate rows. Thus the intensity maxima observed at $\theta_{\mathrm{Fe}} \approx 0.13$ ML can be attributed to the formation of one complete monatomic row at each step-edge as for many other adsorbates [13] in perfect consistency with our coverage calibration. These maxima are observed for low temperatures (175 K) and are still observable up to 500 K. The mobility of the adsorbate on the substrate terrace is thus high enough to allow decoration of the substrate step-edges already at 175 K. Attachment of Fe to the

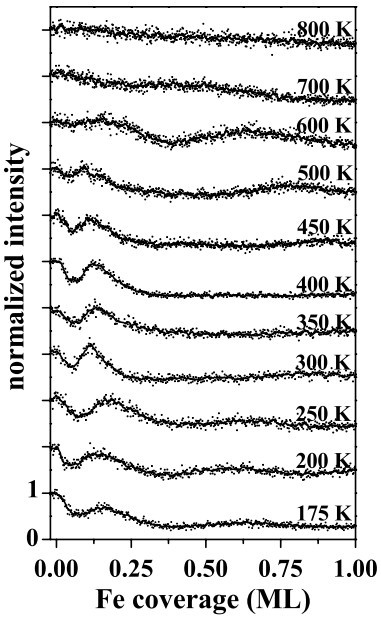

Fig. 2. Normalized reflected He intensity as a function of Fe coverage monitored in situ during deposition at the indicated substrate temperatures. He scattering in grazing geometry, diffraction order $n = 0$, wavelength $\lambda = 0.101$ nm, incidence angle $\theta_i = 85°$ and total scattering angle $\chi = 170°$. For clarity the curves for $T \geqslant 200$ K are vertically shifted by +1 unit for each temperature step.

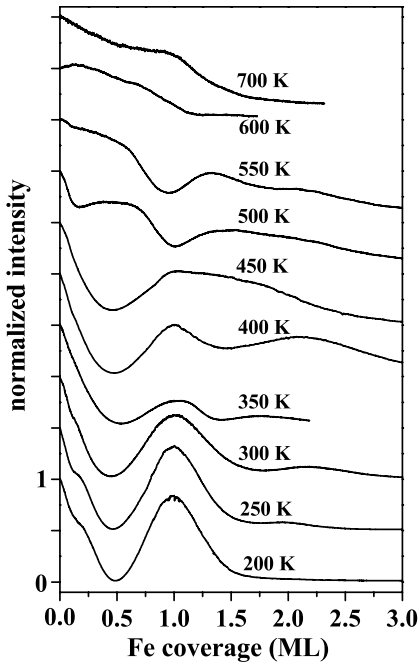

Fig. 3. Normalized reflected He intensity as a function of Fe coverage in non-grazing geometry. He-beam incidence angle $\theta_i = 57.8°$, $\chi = 101.8°$ corresponding to the diffraction order $n = -3$ and specular scattering with respect to the substrate terraces. The presentation is equivalent to the one in Fig. 2 except that for $T \geqslant 250$ K the curves are shifted vertically by multiples of 0.5 units.

Pt(997) step-edge at room temperature has also been observed by scanning tunneling microscopy [6,14].

There is a tendency that below room temperature the maximum of the first peak shifts to coverages larger than 0.13 ML. This can be ascribed to the activation threshold for corner rounding as reported earlier for the cases of Co, Cu, and Ag on Pt(997) [15,16]: Above 250 K, thermal energy becomes comparable to the diffusion barrier between a site in the second Fe row at the step-edge and a site at the uncovered Pt step-edge.

Fig. 3 shows the He reflectivity in non-grazing diffraction geometry measured during Fe deposition at substrate temperatures between 200 K and 700 K. In this scattering geometry information on the morphology and the processes on the terraces can be obtained. This section focusses on the temperature range 200–450 K. A prominent intensity maximum indicates the formation of a complete monolayer before adsorption in the second layer begins. As already stated in Section 2 we use the maximum at 200 K for a consistent coverage and evaporation rate calibration in our study. The deposited amount of Fe at this peak defines the unit 1 ML independent of growth mode changes at higher temperature or coverage. The shoulder at 0.2 ML coverage is again a signature of step decoration. However, in contrast to the data at grazing geometry (Fig. 2) it can not be interpreted in a straightforward manner. The feature in Fig. 3 disappears between $T = 300$ K and $T = 450$ K while Fig. 2 demonstrates that formation of a monatomic row extends to 500 K. At 400 K a second intensity maximum near 2 ML coverage is observed which suggests that layer-by-layer growth continues also in the second layer. The intensity difference between complete and half-completed layer suggests that the growth is, however, only imperfect with a continuous transition to three-dimensional (3D) growth with decreasing temperature. The shift of the second maximum to coverages above 2 ML supports this picture. Further maxima are not observed, except under conditions when the residual gas pressure was unusually high (probably a surfactant induced behavior which was not studied in detail). Due to this behavior we assume that the first Fe layer grows in a pseudomorphic fashion on the Pt terrace although the atomically resolved structure on the terrace could not be assessed due to the large size of the step repeat unit and the small atomic corrugation.

The growth mode established above is corroborated by measurements shown in Figs. 4 and 5. The diffraction scans in Fig. 4 are recorded after depositing the indicated Fe coverages on clean Pt(997) at 350 K. Up to a coverage of 0.71 ML the diffraction peaks of a clean Pt(997) surface are preserved although their intensity decreases with increasing coverage. At 1.5 ML Fe coverage the diffraction pattern has disappeared almost completely and the step–step correlation in the topmost layer is lost. A small peak from (111) regions dominates the pattern. From the peak width it can be concluded that the average size of these regions is not substantially larger than the original terrace width while the regions are not arranged with the strict periodicity of the substrate.

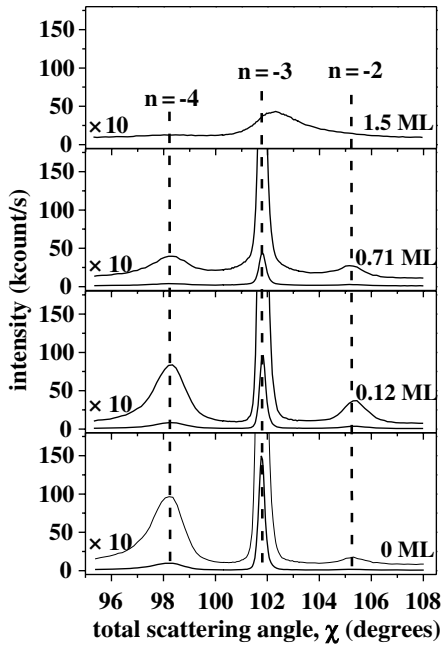

Fig. 4. He diffraction patterns in non-grazing geometry after Fe deposition at $T = 350$ K. The Fe coverage is indicated at each trace. He beam incidence angle $\theta_i = 57.8°$. Peak positions are indicated as dashed lines and correspond to the diffraction orders $n = -4$ to -2.

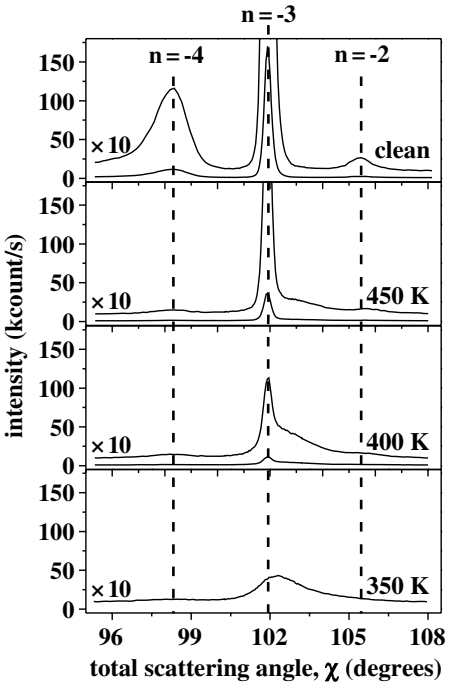

Fig. 5. He diffraction patterns in non-grazing scattering geometry after deposition of 1.5 ML of Fe at $T = 350$ K. The following measurements (bottom to top) were made successively after heating the sample to 400 K and 450 K, respectively. For comparison, the top panel shows the diffraction scan of a well-prepared clean Pt(997) surface. The scattering geometry is the same as for the measurements in Fig. 4.

The sequence of measurements displayed in Fig. 5 starts at the bottom panel with 1.5 ML Fe deposited at 350 K (same as the top panel in Fig. 4) and shows diffraction patterns recorded at 400 K and 450 K after holding the sample for more than 5 min at the respective temperature. By annealing above 400 K the narrow $n = -3$ diffraction peak of the ordered Pt(997) morphology re-appears. The result demonstrates that due to the on-set of diffusion the defect-rich structure formed by Fe deposition at 350 K transforms at 400 K back to an ordered staircase morphology similar to the one of the substrate. This happens exactly at the temperature where a reflectivity maximum slightly above 2 ML coverage is observed (Fig. 3). The growth at low temperature can thus be identified with a Stranski–Krastanov (SK) like growth mode, which around 400 K approaches a layer-by-layer growth mode. The behavior is, however, induced by kinetics rather than by the balance of free surface and strain energies which are the important parameters in regular SK growth. This clearly indicates that the Fe diffusion barrier is much higher on the Fe covered surface than on the Pt substrate resulting in a reduction of step decoration in the second Fe layer and favoring island nucleation on the terraces.

Although helium scattering has no explicit chemical specificity the observed morphological changes at low temperature (200–450 K) suggest that Fe attaches to the step-edges and grows without significant intermixing with the substrate. This is important as we will contrast this point with the effects due to Fe–Pt alloying at higher temperature which will be discussed in Section 3.2. It is known that Pt atoms at the step-edge are mobile already at $T = 400$ K as Pt evaporation on Pt(997) at this temperature proceeds without intensity decrease in grazing helium scattering [17]. Fe incorporation into the substrate terrace e.g. through exchange at the step-edge would expel a Pt atom which can, hence, migrate and attach to an existing kink site. As a result oscillations of defect density at the step-edge would exhibit an increased period when the mobility increases. Assuming such an exchange the maximum would have to occur at a coverage above 0.13 ML and it should shift to higher coverage with increasing temperature. This is, however, in clear contrast to the experimental result.

The formation of the Fe monolayer also suggests the absence of significant Fe–Pt intermixing. For evaporation at $T \leqslant 400$ K the intensity as a function of coverage follows a parabolic curve typical for layer-by-layer growth [18]. The reflectivity decreases to 1.5% of the clean substrate value in the minimum at 0.5 ML Fe coverage and almost fully recovers when 1 ML coverage is reached (Fig. 3). On the other hand, growth occurs by step decoration without extensive defect creation. Thus, the relevant mechanism which reduces the reflectivity must be destructive interference between He waves scattered from areas of different height (denoted as anti-phase scattering) [19]. An estimate of the Fe island height supports this statement. The scattering condition in Fig. 3 exhibits a perpendicular momentum transfer of 78.5 nm^{-1} and thus corresponds to the 3rd diffraction order (in-phase scattering condition) with respect to adjacent substrate terraces of 0.24 nm height difference

(Fig. 1). The height of a pure Fe layer can be estimated to be 0.18 nm assuming pseudomorphic growth on the Pt terraces and conservation of the bcc atomic volume of Fe. The closest anti-phase condition for an island height smaller than the substrate step height corresponds to 0.19 nm height difference (i.e. diffraction order 5/2). Thus, the low helium intensity at half ML coverage could be well explained by an Fe layer whose height is about 0.05 nm smaller than that of a Pt layer.

In summary, the analysis of the data for temperatures below 500 K demonstrates that substrate steps play an important role in the formation of the first monolayer. Fe growth on Pt(1 1 1) is reported to exhibit a three-dimensional growth mode with cluster formation at room temperature and 500 K [5]. Pt(1 1 1) differs from the vicinal substrate used in this study essentially by its much lower step density and much larger average terrace size. The effect of an increased step density is thus to inhibit island nucleation on the Pt terraces and favor the growth of smooth layers by means of preferential step decoration.

3.2. Alloying of Fe with Pt from the Pt(9 9 7) substrate

Fe and Pt exhibit a strong tendency for alloy formation and Fe exhibits antisegregation on Pt surfaces (segregation energy Fe/Pt: +0.63 eV/atom with a strong tendency for mixing [20]). We first discuss the onset of bulk alloying on Pt(9 9 7) using AES.

The experiment is performed as follows: After deposition of 1 ML Fe at $T = 200$ K, the temperature is increased in steps of 50 K or 100 K to $T = 800$ K. After each step the sample temperature is held constant for more than 5 min before an AES spectrum from 20 eV to 770 eV is recorded (primary electron energy 3 keV). The relative amount of Fe near the surface is estimated by [21]

$$C_{\mathrm{Fe}} = \frac{I_{\mathrm{Fe}}}{S_{\mathrm{Fe}}} \cdot \left(\sum_{\alpha=\mathrm{Fe,Pt}} \frac{I_\alpha}{S_\alpha} \right)^{-1}, \qquad (1)$$

where I_α is the peak to peak intensity of a specific Auger line of the element α (α = Fe, Pt), and S_α is the relative sensitivity factor of the elements, namely $S_{\mathrm{Pt}} = 0.025$ and $S_{\mathrm{Fe}} = 0.20$ [21]. In Fig. 6 the Fe concentration near the surface is plotted as a function of temperature using the LMM peak at $E = 651$ eV for Fe and the MNN peak at $E = 64$ eV as a reference. The more surface sensitive 47 eV peak of Fe could not be used due to overlap with other Pt Auger peaks. We find that the relative amount of Fe within the information depth of AES is approximately constant for $T \leqslant 600$ K, then starts to decrease and becomes undetectable above 850 K. We assign the onset of the decrease at 600 K to the beginning of Fe diffusion into the Pt bulk. Thus, Fe deposited on Pt(9 9 7) diffuses into the bulk on a timescale of minutes at temperatures above 600 K.

The continuous decrease of He intensity which occurs above 600 K (see Fig. 3) can thus be attributed to bulk alloying. The shape of the He reflectivity curves at 500 K and 550 K are, however, not accounted for by bulk diffusion. In the following we discuss three possible processes, a structural transition, double layer growth, and surface alloying with respect to their capability to explain the experimental observation.

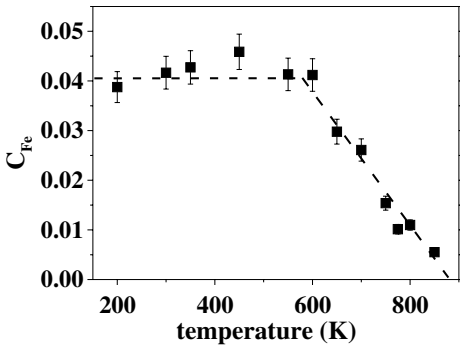

Fig. 6. Concentration of Fe monitored by AES while increasing the sample temperature in steps of 50 K or 100 K. Initially, 1 ML of Fe is deposited at 200 K. The holding time at each temperature is 5 minutes before a spectrum is taken. The relative amount of Fe is obtained from Eq. (1) using peak intensities from Auger spectra (see text). The line is a guide to the eye.

At 500 K and 550 K we may observe a growing Fe monolayer with a different lattice structure than at lower temperature. Due to the lattice mismatch of substrate and adlayer material a change from a commensurate to an incommensurate lattice of the growing adlayer would be probable. The corresponding deviation of calibrated coverage (at low temperature) and actual coverage, however, cannot be larger than 20% based on the difference of nearest neighbor distances of Pt and Fe in their respective bulk crystal structure. The observed change of the reflectivity minimum by 100%, from 0.5 ML Fe coverage at low temperature to 1 ML between 500 K and 550 K, excludes, such a transition. It might, rather, suggest a transition from monolayer growth at low temperature to double layer growth above 500 K. In fact, the anti-phase scattering condition of the single Fe layer height discussed in Section 3.1. would result in an in-phase scattering condition for a double layer in agreement with the observed slow initial decrease for the 500 K reflectivity curve. This growth mode can, however, not explain the abrupt change of slope by a factor of 2 around 0.5 ML coverage. At that point only one quarter of the terrace would be covered by a double layer and layer formation would still be in continuous progress. Moreover, if a Fe double layer is the energetically most favorable structure it would have to occur similarly at step-edges on Pt(1 1 1) which is not observed by STM [3].

In contrast to these morphological transitions, we will show that the formation of a surface alloy is in good agreement with observation and represents the most convincing picture to explain the reflectivity curves in the temperature range 500–550 K in Fig. 3. While Fe diffusion into the Pt bulk is kinetically hindered below 600 K there still exists a strong driving force for Fe to intermix with Pt [20] which

can drive an alloying process within the surface layer because energy barriers at the surface are lower than for diffusion in the bulk. As was shown earlier by calculation [22] and experiment [23] alloying can proceed with an increased rate at step-edges followed by diffusion *within* the terrace. Atoms at the step-edge are more weakly bound due to their lower coordination and they can be easily displaced towards the adjacent terrace.

In Section 3.1. we found that the growth of the Fe layer reduces the reflectivity substantially as it establishes an almost perfect anti-phase scattering condition. At 550 K the growing layer provides, however, only little reflectivity reduction. This suggests that Fe and Pt regions are no more spatially separated but become mixed on an atomic scale so that an effective layer height close to the Pt step height is observed in the interaction with the scattering helium beam. It is evident that a dissolution of adsorbate atoms in the terrace will not be accompanied by He intensity oscillations but will result in a continuous and slow decrease of reflectivity with increasing coverage.

The Fe reflectivity curve recorded at 500 K exhibits a specifically interesting feature (see Fig. 3). At the beginning of Fe deposition we observe a steep decrease then a minimum close to 0.13 ML followed by an intensity recovery until 0.5 ML. Below 0.13 ML the curve follows closely the low temperature behavior, for which no significant alloying occurs as we discussed in Section 3.1. Only during continued Fe deposition the reflectivity increases and approaches the behavior of the 550 K curve. This suggests that the first Fe row decorating the step-edge forms a metastable structure and becomes incorporated into an alloy only during continued Fe deposition.

The first steep reflectivity decrease observable at 500 K and 550 K starts only at a Fe coverage above 0.5 ML. A minimum is found at 1 ML, and a high reflectivity is attained again around 1.5 ML. This resembles the parabolic intensity behavior observed at low temperature between 0 ML and 1 ML coverage, shifted, however, by 0.5 ML to higher coverage. It suggests that for deposition beyond 0.5 ML a Fe monolayer grows on top of the alloy. The low minimum reflectivity at 1 ML is again characteristic for the Fe layer height and not for a Pt or alloy layer. In comparison to growth on a clean and annealed substrate the onset of the parabola at 0.5 ML is not sharp but smooth due to inhomogenities created by the initial Fe deposition.

It cannot be decided if layer-by-layer growth on top of the alloy continues beyond one monolayer because the reflectivity curves show no additional pronounced oscillations. The slowly decreasing reflectivity may indicate either a step flow growth with increasing defect concentration due to the presence of the substrate steps or an island growth with increased inter-layer diffusion.

The 0.5 ML offset for beginning Fe layer growth indicates that the formed alloy monolayer is completed at a Fe coverage of 0.5 ML which corresponds nominally to a $Fe_{50}Pt_{50}$ alloy. In fact, an alloy with this stoichiometry is known to be readily formed at higher temperature on Pt(1 1 1) and orders in alternating rows of Pt and Fe [8]. We remark that for the surface of an alloy crystal, namely $Pt_{80}Fe_{20}$(1 1 1), substantial depletion of Fe in the top layers was found for temperatures above 700 K [24,25]. In contrast, Fe deposited on Pt(1 1 1) at room temperature followed by annealing between 600 K and 850 K is known to form an ordered surface alloy within the top-most layer containing almost 50% of Fe [7]. We suggest that the surface alloy formed on Fe/Pt(9 9 7) exhibits a structure similar to the (1 1 1) plane of the bulk $L1_0$ $Pt_{50}Fe_{50}$ alloy [8]. A search for superstructure peaks in He diffraction which could arise from an ordered double row periodicity was not successful. However, even the diffraction peaks of the Pt corrugation cannot be identified within the background counting rate for the preparation conditions of surface alloying. Also in low energy electron diffraction (LEED) superstructure peaks were not observable. This is, however, not surprising since already on a Pt(1 1 1) substrate the LEED superstructure peaks of the FePt alloy are substantially broadened [7]. The large repetition unit of Pt(9 9 7) and the deviations from perfect periodicity of the step array make the observation of local order inside a terrace even more difficult. The absence of observable superstructure peaks can, in fact, be expected if chemical order extends only over distances of a few nm. For comparison, the FePt alloy on Pt(1 1 1) exhibits domains of parallel Fe rows alternating with Pt rows with a strong tendency for local ordering but a high density of domain walls between antiphase domains and domains of different azimuthal row orientation [8,26].

3.3. Alloying kinetics

The surface morphology obtained at temperatures below 500 K which can be attributed to the growth of a Fe monolayer does not correspond to the equilibrium morphology of the system. We demonstrate this by stopping the deposition at different Fe coverages below 0.2 ML, i.e. in the steeply decreasing part of the reflectivity curve. When we monitor the following increase of the He reflectivity as a function of time, we can study the alloying kinetics.

Fig. 7 reproduces the continuous Fe deposition curves at 450 K and 550 K from Fig. 3. The corresponding Fe coverage is given in the upper scale. In addition, we present deposition curves at the intermediate temperature 475 K which initially closely follow the 450 K curve. Upon stopping the Fe deposition at (a) 0.06 ML, (b) 0.13 ML, and (c) 0.19 ML the system starts to relax towards equilibrium which results in an increase of He intensity. The relaxation curves can be approximated by a single exponential fit (solid lines in Fig. 7). The recovery tends for long times towards a reflectivity which reduces for increasing Fe coverages. The fully relaxed reflectivity based on the fits does not exceed the value on the 550 K curve at the same Fe coverage marked in Fig. 7 as a_∞, b_∞, and c_∞, respectively.

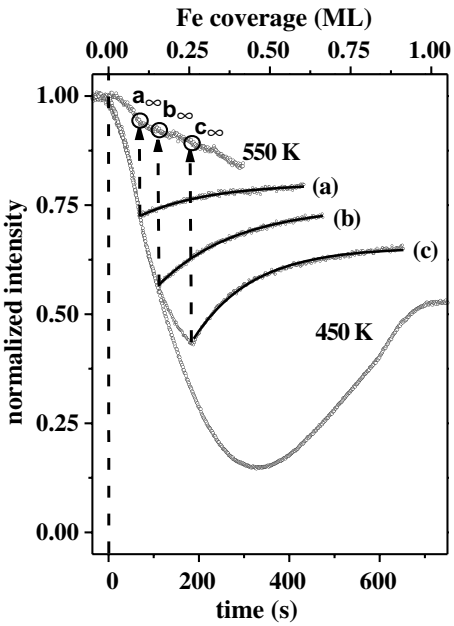

Fig. 7. Deposition of Fe (coverage scale, top) and recovery of reflected He intensity (time scale, bottom). In the curves (a)–(c) Fe is deposited at 475 K at a deposition rate of 0.0014 ML/s. When deposition is stopped at the coverages (a) 0.06 ML, (b) 0.13 ML, and (c) 0.19 ML the slope changes sign and the reflectivity recovers. The solid lines in the curves (a)–(c) are single exponential fits. For comparison we show the deposition curves at 450 K and at 550 K, both taken from Fig. 3. For all curves the scattering geometry is the same as in Fig. 3.

This demonstrates that relaxation at 550 K is instantaneous on the experimental time scale. In contrast, adsorption curves recorded between 450 K and 550 K are determined by the interplay of Fe deposition rate and alloying.

Compared to a trace of reflectivity during a heating-and-cooling-cycle the data presented in Fig. 7 which are obtained at constant temperature have the advantage to demonstrate not only the irreversible relaxation towards equilibrium but also the temperature dependence of relaxation time. Moreover, we can thus reduce any effects due to superposition with Fe bulk diffusion which occurs at slightly higher temperature.

From the fitted single exponentials (Fig. 7) a recovery time (1/e value of the exponential fit) of $150\text{ s} \pm 20\text{ s}$ is found at 475 K. Within experimental precision the time constant is independent of Fe coverage. Corresponding measurements at different temperature (not shown) indicate a variation from recovery times longer than 300 s at 450 K to recovery times shorter than 100 s at 500 K. With respect to the time required to deposit one Fe row the recovery at 450 K is thus still slow while it is already fast at 500 K. This suggests a substantial activation energy. Using an Arrhenius model we estimate an effective activation energy of 0.7 ± 0.3 eV. This energy may be related to the barrier height, either for the Pt–Fe exchange or the diffusion of Fe atoms (or the accompanying vacancies) inside the terraces.

Earlier studies show that step-edge specific processes are the key to an increase of diffusion into the topmost substrate layer thus resulting in a lowered onset temperature of alloying. For Ni/Cu(1 1 1) Raeker et al. [22] find strongly enhanced alloying through processes involving adsorbate incorporation at the step-edge due to two channels: adsorbate atoms burrowing into the terrace and pushing out substrate atoms, and diffusion into the terrace from an adsorption site at the lower step-edge. In an STM study of Ni/Pt(9 9 7) [23] alloying is even observed at temperatures as low as 150 K due to an efficient alloying pathway involving the step-edge.

Finally, the results presented in this paper shall be compared to a study of Fe deposited on the low index Pt(1 1 1) by Jerdev et al. [7]. The study focuses on chemical surface composition for Fe coverages around 1.5 ML analyzed by low energy ion scattering, X-ray photoelectron spectroscopy, and LEED. Although both, the study by Jerdev et al. and ours, find a similar sequence of surface structures there are characteristic differences. Jerdev et al. [7] find an alloy of stabilized composition (45% Fe) at the surface over the temperature range 600–850 K whereas we assign the measurements at 500 K and 550 K to the formation of a FePt monolayer alloy containing approximately 0.5 ML Fe. The temperature ramps in their study are run on a shorter time scale (10 s dwell time) than the experiments presented here (typical dwell times of more than 5 min). In addition, in their study Fe is deposited before the sample is annealed to a given temperature while in our study Fe is deposited at the observation temperature. The different experimental procedures may result in a lower temperature of alloy formation in our study. The substantial difference of more than 100 K between the studies suggests, however, that the decisive reason is the different step density. In comparison to the Pt(1 1 1) surface the vicinal surface provides a high density of high coordination sites for adsorbing atoms already at low adsorbate coverage and thus provides additional and efficient paths leading to alloying. The residence time of single adatoms on the terraces is reduced with respect to Pt(1 1 1) and their attachment to steps is enforced especially for coverages below 1 ML. The lowering of the observed alloying temperature thus suggests a more efficient alloying process for Fe through the Pt step-edge with respect to Fe on terrace sites or at the edges of Fe islands.

4. Conclusion

We investigated the Fe growth on the vicinal Pt(9 9 7) surface in situ by thermal energy He scattering. The results are summarized graphically in Fig. 8. We find Fe layer growth starting from step decoration between 200 K and 450 K. A strongly modified growth behavior at 500 K and 550 K can be assigned to the formation of a surface restricted alloy. Bulk alloying occurs for $T \geqslant 600$ K which is shown by Auger electron spectroscopy. Comparison of our results to studies on the growth of Fe on Pt(1 1 1)

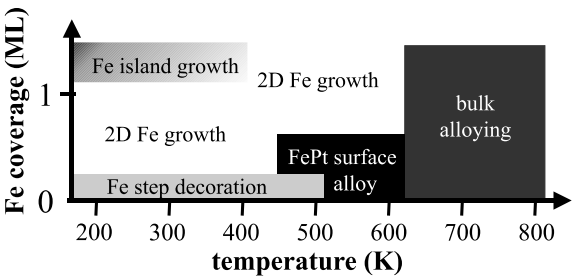

Fig. 8. Growth modes of Fe on Pt(997) as a function of temperature at a deposition rate around 10^{-3} ML/s.

demonstrates that a low step density provides a rough film morphology whereas the vicinal surface employed in this study promotes formation of a flat monolayer and suppresses three-dimensional growth at least up to monolayer completion. Bulk and surface alloy formation occur on both, flat and vicinal surfaces but become activated at temperatures which are 100–150 K lower on the vicinal surface.

This study allows to derive three specific recipes to prepare nanometer-sized structures: (1) Perfect decoration of the step-edges of Pt(997) by monatomic Fe chains occurs between 250 K and 500 K. (2) The best order of a Fe ML as judged from the He reflectivity is obtained around $T = 400$ K. (3) The FePt mixing remains restricted to the surface layer if Fe is evaporated between 500 K and 550 K.

Acknowledgements

One of the authors (T.-Y. Lee) acknowledges financial support from the Korean Ministry of Education and Human Resources Development through the program of the Brain Korea 21 through Materials Education and Research division in Seoul National University.

References

[1] T.C. Hufnagel, M.C. Kautzky, B.J. Daniels, B.M. Clemens, J. Appl. Phys. 85 (1999) 2609.
[2] M. Abid, H. Lassri, R. Krishnan, M. Nývlt, S. Visnovský, J. Magn. Magn. Mater. 214 (2000) 99.
[3] M. Ritter, W. Ranke, W. Weiss, Phys. Rev. B 57 (1998) 7240.
[4] Y.J. Kim, C. Westphal, R.X. Ynzunza, Z. Wang, H.C. Galloway, M. Salmeron, M.A. Van Hove, C.S. Fadley, Surf. Sci. 416 (1998) 68.
[5] W. Weiss, M. Ritter, Phys. Rev. B 59 (1999) 5201.
[6] R. Cheng, K.Y. Guslienko, J.Y. Fradin, J.E. Pearson, H.F. Ding, D. Li, S.D. Bader, Phys. Rev. B 72 (2005) 014409.
[7] D.I. Jerdev, B.E. Koel, Surf. Sci. 513 (2002) L391.
[8] M. Schmid, P. Varga, Segregation and surface chemical ordering - an experimental view on the atomic scale, in: D.P. Woodruff (Ed.), The Chemical Physics of Solid Surfaces, vol. 10, Elsevier, 2002.
[9] P. Gambardella, A. Dallmeyer, K. Maiti, M.C. Malagoli, W. Eberhardt, K. Kern, C. Carbone, Nature 416 (2002) 301.
[10] P. Gambardella, A. Dallmeyer, K. Maiti, M.C. Malagoli, S. Rusponi, P. Ohresser, W. Eberhardt, C. Carbone, K. Kern, Phys. Rev. Lett. 93 (2004) 077203.
[11] M. Blanc, K. Kuhnke, V. Marsico, K. Kern, Surf. Sci. Lett. 414 (1998) L964.
[12] E. Hahn, H. Schief, V. Marsico, A. Fricke, K. Kern, Phys. Rev. Lett. 72 (1994) 3378.
[13] V. Marsico, M. Blanc, K. Kuhnke, K. Kern, Phys. Rev. Lett. 78 (1997) 94.
[14] T. Y. Lee, P. Wahl, A. M. Schneider, K. Kuhnke and K. Kern, (unpublished).
[15] P. Gambardella, M. Blanc, H. Brune, K. Kuhnke, K. Kern, Phys. Rev. B 61 (2000) 2254.
[16] P. Gambardella, M. Blanc, L. Bürgi, K. Kuhnke, K. Kern, Surf. Sci. 449 (2000) 93.
[17] K. Kuhnke, K. Kern, J. Phys.: Cond. Matter 15 (2003) S3311.
[18] B. Poelsema, G. Comsa, Springer Tracts in Modern Physics, vol. 115, Springer-Verlag, 1989.
[19] B. Poelsema, A.F. Becker, G. Rosenfeld, R. Kunkel, N. Nagel, L.K. Verheij, G. Comsa, Surf. Sci. 272 (1992) 269.
[20] A. Christensen, A.V. Ruban, P. Stoltze, K.W. Jacobsen, H.L. Skriver, J.K. Nørskov, F. Besenbacher, Phys. Rev. B 56 (1997) 5822.
[21] L.E. Davis, N.C. MacDonald, P.W. Palmberg, G.E. Riach, R.E. Weber, Handbook of Auger Electron Spectroscopy, Perkin-Elmer Corp., 1978.
[22] T.J. Raeker, A.E. DePristo, J. Vac. Sci. Technol. A 10 (1992) 2396.
[23] P. Gambardella, K. Kern, Surf. Sci. 475 (2001) L229.
[24] P. Beccat, Y. Gauthier, R. Baudoing-Savois, J.C. Bertolini, Surf. Sci. 238 (1990) 105.
[25] C. Creemers, P. Deurinck, Surf. Interf. Anal. 25 (1997) 177.
[26] D. Payer, CO-Adsorption auf PtFe-Legierungsschichten, Diploma Thesis; Technische Universität Wien, 2001.